arXiv:2105.01913v1 [cs.SI] 5 May 2021

Optimally partitioning signed networks based on generalized balance

Samin Aref[1]* and Zachary P. Neal[2]

[1]Max Planck Institute for Demographic Research, 18057 Rostock, Germany
[2]Department of Psychology, Michigan State University, East Lansing, MI 48824, USA

*To whom correspondence should be addressed; E-mail: sare618@aucklanduni.ac.nz

Abstract

Signed networks, which contain both positive and negative edges, are now studied in many disciplines. A fundamental challenge in their analysis is partitioning the nodes into internally cohesive and mutually divisive clusters based on generalized balance theory. However, identifying optimal partitions is NP-hard. We introduce a binary linear programming model, and reformulate an existing one, to solve this challenge by minimizing the number of "frustrated" (intra-cluster negative or inter-cluster positive) edges. These models make it possible to partition a signed network into exactly k clusters that minimize the number of frustrated edges, and to identify the smallest number of clusters that minimizes the number of frustrated edges across all possible partitions. They guarantee an optimal solution, and can be practically applied to signed networks containing up to 30,000 edges, and thus offer a robust method for uncovering the structure of signed networks. We demonstrate the practicality and utility of these models by using them to identify optimal partitions of signed networks representing the collaborations and oppositions among legislators in the US House of Representatives between 1981 and 2018. We show that an optimal partition into three coalitions better describes these networks than a partition based on political party. The optimal 3-partition reveals a large liberal coalition, a large conservative coalition, and a previously obscured third coalition. This hidden third coalition is noteworthy because its median ideology changes over time, but its members are consistently more effective at passing legislation than their colleagues in either of the dominant coalitions.

Keywords: Signed graph, optimal partition, balance theory, weak balance, optimization, mathematical modeling, US Congress, House of Representatives, legislative effectiveness

Introduction

Signed networks, in which nodes can be connected by positive or negative relationships, occur in many contexts. To identify communities in signed networks it is often useful to put the nodes into clusters so that most positive relationships are within clusters, while most negative ties are between clusters. Identifying clusters of nodes that optimally meet these criteria is computationally challenging, but we present feasible methods for doing so. Applying these new global optimization methods to signed networks of the US House of Representatives shows that legislators are actually organized into three coalitions whose ideological composition offers new insights on the otherwise obscured interplay between partisanship and legislative effectiveness.

Signed networks are studied in a diverse range of contexts in both the natural [1, 2, 3] and social [4, 5, 6, 7] sciences. Across these contexts, it is often of interest to identify clusters of nodes that are internally cohesive and mutually divisive, and thus partially satisfy the conditions of *generalized balance* [8, 9, 10, 11]. However, identifying an optimal partition of nodes into such clusters involves solving fundamental non-deterministic polynomially acceptable hard (NP-hard) optimization problems [12, 13, 14].

A common misconception about solving NP-hard optimization problems is that "only heuristic methods" [15, page 3] can be used for them. Previous works in this area have used a modified the concept of network *modularity* to incorporate signed edges [16, 15]. They used a *Tabu search* heuristic algorithm on a signed network with 1131 edges [16] and used a *simulated annealing* heuristic algorithm on a signed network with 2517 edges [15], in each case settling for sub-optimal partitions whose distance from optimality remains unknown. Unlike modularity, the concept of *frustration* [17, 18] requires no modification for application in signed networks because it originates from Ising models of atomic magnets in which couplings of opposite nature exist [19]. Using frustration and two mathematical optimization models, we propose and demonstrate a general method for finding a *globally optimal* partition of signed networks with up to $30,000$ edges.

Identifying an optimal partition of nodes into internally cohesive and mutually divisive clusters involves two computational challenges. The first challenge is finding a k-partition of a signed network, placing nodes into k clusters that minimize intra-cluster negative and inter-cluster positive edges (*frustrated edges*), where k is selected in advance [14]. A second challenge is finding the smallest number of clusters k^*_{min} that minimizes frustrated edges among all partitions across all values of k. These challenges are unique from, but conceptually analogous to related challenges in community detection in unsigned networks: It is difficult to find a modularity maximizing partition into a specific number of clusters, but even harder to find the modularity maximizing partition into any number of clusters [20]. We solve the first challenge by generalizing a mathematical programming model for finding an optimal 2-partition [18, 14, 21] and introducing a generalized model to find optimal k-partitions. Then, we tackle the second challenge by reformulating another mathematical model [13] for non-complete graphs and solving it without providing the number of clusters.

We demonstrate the practicality of these methods, and illustrate how they can generate novel

insights, by applying them to signed networks of political collaboration and opposition in the US House of Representatives from 1981 to 2018. Research on and descriptions of the US House usually place legislators into clusters defined by legislators' political party affiliations. However, reliance on a simple binary attribute risks oversimplifying this complex system because it ignores information about the positive and negative interactions between individual legislators. We explore whether placing legislators into optimal clusters defined by their interactions, rather than simply by their parties, better captures the coalitional structure of the chamber. We find that the best fitting parsimonious solution places legislators into three clusters characterized by a large liberal coalition, a large conservative coalition, and a smaller ideologically fluid coalition. Interestingly, we find that members of this ideologically fluid third coalition are substantially more effective at passing legislation than members of either dominant coalition. These findings suggest that, although political parties are clearly influential in US politics, some of the heavy lifting in the US House is done by a small splinter coalition of highly effective legislators who are ideologically aligned, but not necessarily collaborating, with members of the majority party's core.

Partitioning signed networks

Preliminaries

A *signed network* is an undirected simple graph with positive and negative signs on the edges usually denoted as $G = (V, E, \sigma)$ where V and E are the sets of nodes and edges respectively, and σ is the sign function $\sigma : E \rightarrow \{-1, +1\}$. Graph G contains $|V| = n$ nodes and its symmetric signed adjacency matrix is denoted by $\mathbf{A}$. The set E of edges contains m^- negative edges and m^+ positive edges adding up to a total of $|E| = m = m^+ + m^-$ undirected signed edges. An edge with endpoints i and j is represented by (i, j) such that $i < j$. Given a signed graph $G = (V, E)$, a *k-partition* is a division of the nodes V into k non-empty subsets $V_1, V_2, \ldots, V_k$ such that $V_i \cap V_j = \varnothing \forall i \neq j$ and $\cup_{i=1}^{k} V_i = V$ (i.e. every node belongs to exactly one subset).

Balance theory was conceptualized in the 1940s in the context of social psychology [22], recast in graph theoretic terms in the 1950s [23], and generalized in the 1960s [8]. Whereas classic balance holds that a signed network can be partitioned into up to two clusters [23], generalized balance holds that it can be partitioned into any number of clusters, which allows a more flexible structural decomposition of networked systems, which in turn offers a more nuanced view of polarization in social and political systems [24, 25, 26]. According to generalized balance theory, a signed network is *k-balanced* (i.e. *clusterable*) if its nodes can be partitioned into k clusters (or "coalitions" [27]) such that each positive edge joins nodes belonging to the same cluster, and each negative edge joins nodes belonging to different clusters [8]. Edges that fail to meet these criteria (i.e. a negative edge within a cluster, or positive edge between clusters) are called *frustrated* edges under that partition.

Generalized balance in empirical signed networks can be analyzed by measuring their distance to clusterability [9, 11, 14]. The distance of a given network G to clusterability can be quantified as the minimum number of frustrated edges for all possible partitions into k clusters [11, *k-clusterability index* $C_k(G)$], or the minimum number of frustrated edges among all possible partitions with any number of clusters $1 \leq k \leq n$ [9, *clusterability index* $C(G)$]. Obtaining these measures require intensive computation and are NP-hard [12].

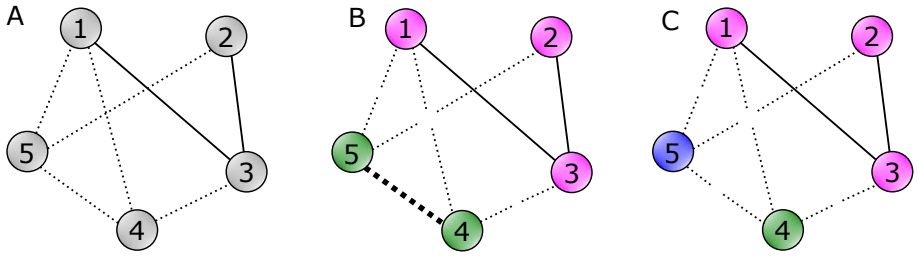


Figure 1: (A) An example signed network. (B) Evaluating classic balance via bi-partitioning. (C) Evaluating generalized balance and clusterability via k-partitioning

Fig. 1(A) shows an example signed network with five negative edges (dotted lines) and two positive edges (solid lines). The signed network can be optimally partitioned into two clusters based on classic balance (B), or three clusters based on generalized balance (C). The classic approach leads the 2-partition $\{\{1,2,3\},\{4,5\}\}$ (shown by green and purple colors in Fig. 1B) which minimizes the total number of intra-cluster negative and inter-cluster positive edges to $C_2(G) = 1$. The generalized approach, (Fig. 1C), leads to the 3-partition $\{\{1,2,3\},\{4\},\{5\}\}$ which satisfies the conditions of generalized balance ($C(G) = C_3(G) = 0$).

Finding an optimal k-partition and the k-clusterability index

We formulate an optimization model that computes the k-clusterability index of an input signed network in its optimal objective function. In a given feasible solution of the optimization problem, each node belongs to one of a set of k clusters $C = \{1, 2, \ldots, k\}$. The binary decision variable x_{ic} takes the value 1 if node $i \in V$ belongs to cluster $c \in C$ (and $x_{ic} = 0$ otherwise).

We consider that a positive edge $(i,j) \in E^+$ is frustrated (indicated by $f_{ij} = 1$) if its endpoints i and j are in different clusters; otherwise it is not frustrated (indicated by $f_{ij} = 0$). A negative edge $(i,j) \in E^-$ is frustrated (indicated by $f_{ij} = 1$) if its endpoints i and j are in the same cluster; otherwise it is not frustrated (indicated by $f_{ij} = 0$).

Using the binary decision variable x_{ic}, we formulate the process to find an optimal k-partition and compute the k-clusterability index as the binary linear programming model in (1). The model in (1) is an extension of a model based on classic balance which provides an optimal 2-partition and computes the 2-clusterability index (a.k.a. the frustration index) of a

signed network [18, 14].

$$
\begin{aligned}
\min \quad & \sum_{(i,j)\in E} f_{ij} \\
\text{s.t.} \quad & \sum_{c\in C} x_{ic} = 1 \quad \forall i \in V \\
& f_{ij} \geq x_{ic} - x_{jc} \quad \forall (i,j) \in E^+,\ \forall c \in C \\
& f_{ij} \geq x_{ic} + x_{jc} - 1 \quad \forall (i,j) \in E^-,\ \forall c \in C \\
& x_{ic} \in \{0,1\} \quad \forall i \in V,\ \forall c \in C \\
& f_{ij} \in \{0,1\} \quad \forall (i,j) \in E
\end{aligned}
\tag{1}
$$

The objective function in (1) computes the minimum number of frustrated edges among all k-partitions. The first constraint in (1) ensures that each node belongs precisely to one cluster. The second and third constraints formulate the relationship between frustration of an edge (left-hand side) and the cluster membership of the endpoints of that edge (right-hand side) respectively for positive edges and negative edges.

Finding an optimal partition and the clusterability index

The more general problem of finding an optimal partition without specifying k and computing the clusterability index of a signed network G is known as the Correlation Clustering problem [12, 28, 29]. We reformulate the mathematical model initially proposed in [13] which is defined in the context of complete networks and widely used in the literature [29, 30, 31, 32] as follows. For every pair of nodes $i, j, i < j$, we define the binary decision variable y_{ij} which takes the value 1 if i and j belong to the same cluster and takes the value 0 otherwise. The model in (2) uses these binary variables to count the frustrated edges in the objective function. In (2), the term a_{ij} represents the entry of the input graph's adjacency matrix $\mathbf{A}$ associated with the pair of nodes $i, j \in V$. To efficiently handle possibly non-complete networks, we use the set T for the constraints of the model in (2). $T = \{(i,j,k) \in V^3 \mid |a_{ij}| + |a_{ik}| + |a_{jk}| \geq 2, i < j < k\}$ denotes the set of all connected triads (node triples connected by at least two edges) in G.

$$
\begin{aligned}
\min \quad & \sum_{i\in V} \sum_{j\in V, j>i} a_{ij}((a_{ij}+1)/2) - a_{ij} y_{ij} \\
\text{s.t.} \quad & y_{ij} + y_{ik} \geq 1 + y_{jk} \quad \forall (i,j,k) \in T \\
& y_{ij} + y_{jk} \geq 1 + y_{ik} \quad \forall (i,j,k) \in T \\
& y_{ik} + y_{jk} \geq 1 + y_{ij} \quad \forall (i,j,k) \in T \\
& y_{ij} \in \{0,1\} \quad \forall i \in V,\ j \in V,\ i < j
\end{aligned}
\tag{2}
$$

Although we use both models in (1)–(2), they are not necessarily dependent. Under the assumption that $k <<< n$, our proposed model in (1) is less computationally intensive than

the model proposed by [13], which we have reformulated in (2). Despite similar scaling of the number of variables with $\mathcal{O}(n^2)$, constraints of (1) have a quadratic growth with $\mathcal{O}(n^2)$ while constraints of (2) have a cubic growth $\mathcal{O}(n^3)$.

These models can be used for partitioning any signed network into internally cohesive and mutually divisive clusters based on generalized balance theory. Their main advantage against existing methods [12, 13, 30, 31, 32] is that they can be practically solved exactly to produce globally optimal solutions for networks of considerable size. In the next section we demonstrate their practicality in networks with up to $30,000$ edges. We solve the optimization models in (1) and (2) to global optimality using *Gurobi* solver (version 9.1) [33] on a virtual machine with 32 Intel Xeon CPU E7-8890 v3 @ 2.50 GHz processors running 64-bit Microsoft Windows Server 2019 R2 Standard.

Partitioning the US House networks

Optimal coalitions

We compare several ways to partition US House legislators into clusters or "coalitions" [27], with the goal of determining the optimal number and the composition of these coalitions. The fitness of a given partition is indicated by its associated number of frustrated edges. The conventional method is to partition legislators into coalitions based on their party affiliations, while here we also explore partitioning legislators into coalitions by applying the optimization models in (1)–(2) to signed networks of their collaborations and oppositions. Throughout our application of these models in the US House context, we use the term "coalition" to refer to the clusters of legislators within a partition, however the partition is obtained, not only because it is commonly used in political contexts, but also because it was the term suggested for signed network partitions by Harary and Kabell [27]. Legislators' memberships in these coalitions depend on either an attribute (e.g. their political party affiliation) or the solution to (1)–(2), but does not necessarily imply their cohesion with other members of the same coalition.

Fig. 2 illustrates the number of frustrated edges (y-axis) for partitions based on party affiliations and optimal k-partitions for $k \in \{2, 3, \ldots, 7\}$ (x-axis) in signed US House networks (see *SI* Table 1). The number of frustrated edges for a party-based partition (denoted by $C_{\text{party}}(G)$) is considerably larger than that of an optimal 2-partition. This implies that defining coalitions simply in terms of legislators' party affiliations leads to many frustrated edges, and therefore to a poor description of the coalition structure of the chamber. The number of frustrated edges decreases further from $k = 2$ to $k = 3$, which implies that defining coalitions in terms of classic balance still leads to many frustrated edges and thus a poorer fit than defining coalitions in terms of generalized balance. For $k > 3$ there is only marginal decline, and then stagnation, in the number of frustrated edges. Substantively, these results suggest that the signed US House networks are better described by a partition into $k > 2$ coalitions than by a more conventional partition into only two coalitions.

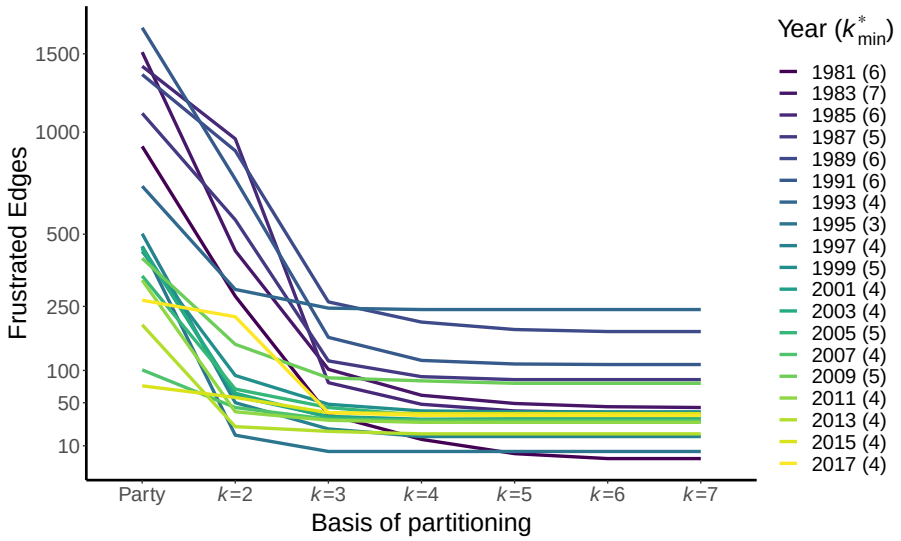


Figure 2: Number of frustrated edges (y-axis) of signed US House networks partitioned using different criteria (x-axis). Each line represents a single network, corresponding to a session of the US House starting in the given year. Fewer frustrated edges indicate that the partition is more consistent with the ties of collaboration and opposition between legislators.

Fig. 2 also reveals the changes over different eras of the House (e.g. sessions with start years 1981-1993 in darker blue-purple shades and 2003-2017 sessions in lighter green-yellow shades). Party-based partitions offer a better fit (i.e. fewer frustrated edges) in recent sessions than in earlier sessions due to increases in partisanship [5, 34, 21]. However, despite changes in the level of partisanship over time, for every session $C_{\text{party}}(G) > C_2(G) > C_3(G)$.

Because the results from Fig. 2 only cover a small range of k, a natural question is whether the fit could be improved further by using larger values of k. Finding the answer is not practically feasible using only the model in (1). Therefore, we solve the model in (2) to find the minimum number of frustrated edges, $C(G)$, across all possible partitions for all possible values of $1 \leq k \leq n$. By juxtaposing $C_k(G)$ from (1) and the values of $C(G)$ from (2), we determine whether the low-points observed in Fig. 2 represent the clusterability indices $C(G)$ of the networks or the number of frustrated edges could decline further for $k > 7$. Through this comparison, we verify that further decline in the frustrated edges is not possible because among all 19 networks, $C(G) = C_k(G)$ at $k \leq 7$. The legend of Fig. 2 shows for each network the exact *point of stagnation* k^*_{min}, which is the smallest number of clusters that minimizes the k-clusterability index across all values of k: $k^*_{\text{min}} = \arg\min_{1 \leq i \leq n} C_i(G)$.

Coalition ideology

Having identified several ways to assign legislators to coalitions in the US House, including optimal k-partitions and optimal partitions, we now examine the ideological compositions of

coalitions defined from three perspectives: party, classic balance ($k = 2$), and generalized balance ($k = 3$). Although we found that $3 \leq k^*_{\text{min}} \leq 7$, in the remaining substantive analyses we focus on the 3-partition in the generalized balance case because $k > 3$ offers only small improvements in fit and therefore $k = 3$ offers a reasonable trade-off between fit and parsimony (See *SI* Figures 5 & 6). Fig. 3 displays the distribution of coalition members' ideology, for each method of defining coalitions (See *SI* Table 2). Coalitions with left-leaning liberal ideologies are shaded blue, while coalitions with right-leaning conservative ideologies are shaded in red; the solid vertical lines indicate a coalition's median ideology.

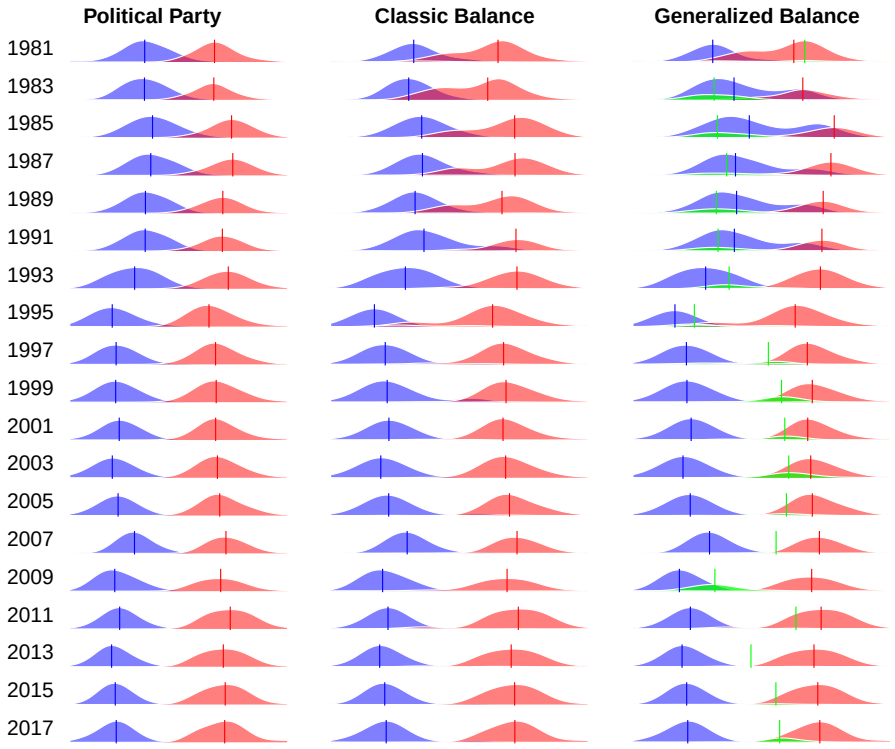


Figure 3: Distribution of coalition members' ideology in the US House of Representatives. Blue (red) curves indicate the ideologies of Democrats (Republicans) in the left column and that of the dominant liberal (conservative) coalitions in the center and right columns. In the right column, green curves indicate the ideologies of members of the smallest coalition.

Partitioning legislators into coalitions based on their political party affiliations (Fig. 3, left column) is the conventional approach in political science, and here displays the familiar pattern of increasing ideological polarization. Partitioning legislators based on classic balance (Fig. 3, center column) offer a more data-driven classification because legislators' coalition memberships are based on their collaborative and oppositional interactions, but is still restrictive because it allows a maximum of two coalitions. The classic balance coalitions display similar ideological distributions to those based on political party: increasing liberal-conservative

ideological polarization.

Partitioning legislators into 3 coalitions based on generalized balance (Fig. 3, right column) also offers a data-driven classification, but allows more nuance. Like the other partitions, the generalized balance partition is characterized by a large liberal coalition and and a large conservative coalition that diverge over time. However, it also includes a smaller and ideologically fluid coalition shaded in green. In the 435-member chamber, this 'third coalition' ranges in size from only 4 members in the 113$^{\text{th}}$ session (2013) to 69 members in the 111$^{\text{th}}$ session (2009). It also ranges in ideology from very liberal in the 98$^{\text{th}}$–102$^{\text{nd}}$ sessions (1983–1991), to center-left in the 103$^{\text{th}}$ and 111$^{\text{th}}$ sessions (1993 and 2009), to center-right in the 105$^{\text{th}}$–110$^{\text{th}}$ sessions (1997–2007).

Coalition effectiveness

The primary task of legislators is to pass laws, and their ability to do so is referred to as *legislative effectiveness* [35, 36, 37]. Therefore, we examine the legislative effectiveness of coalitions in the US House of Representatives, again considering coalitions defined from three perspectives: party, classic balance ($k = 2$), and generalized balance ($k = 3$). Fig. 4 displays coalition members' mean effectiveness, for each method of defining coalitions (See *SI* Table 2). The left-leaning liberal coalition shown as a blue line and the right-leaning conservative coalition shown as a red line. Gray bands illustrate the 95% confidence interval around each estimate, while the blue (Democrat) and red (Republican) backgrounds indicate the majority party in a given session.

Coalitions based on political parties (Fig. 4, top panel) illustrate an expected pattern [38]: the majority party is most effective. This occurs not only because the majority party has more votes, but because it controls key procedural details of the chamber including deciding which bills will come for a vote and when (i.e. agenda-setting power [37]). Coalitions based on classic balance (Fig. 4, center panel) display essentially the same pattern.

Coalitions based on generalized balance (Fig. 4, bottom panel) also display a similar pattern, but with important differences. The large liberal coalition is still more effective when Democrats hold the majority, while the large conservative coalition is still more effective when Republicans hold the majority. However, these two dominant coalitions are both less effective than their party- or classic balance-defined counterparts. These lower levels of effectiveness are explained by the inclusion of the third coalition, shown as a green line, which is the most effective coalition in most sessions. The size and color of the dots along this green line indicate the third coalition's size and median ideology, and highlight that members of the third coalition usually are ideologically aligned with the majority party.

During transitional periods when the majority party changed, members of the third coalition are temporarily less effective. However, during periods of stable party control [39], the highly effective third coalition has been anchored by a small number of consistent and ultra-effective members. For example, the liberal-leaning third coalition during the Democratic-controlled 99$^{\text{th}}$–102$^{\text{nd}}$ sessions (1985–1990) was anchored by Rep. Pat Williams (D-MT1, mean effective-

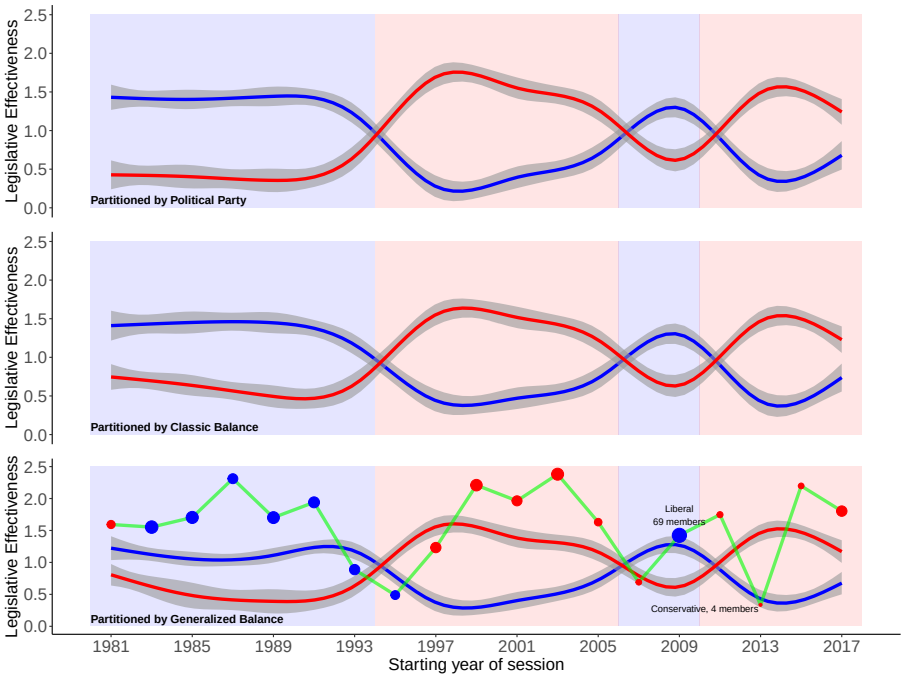


Figure 4: Mean of coalition members' legislative effectiveness in the US House of Representatives. Blue (red) lines indicate the mean legislative effectiveness of Democrats (Republicans) in the top panel and that of the dominant liberal (conservative) coalitions in the center and bottom panels. In the bottom panel, the green line indicates the mean ideological effectiveness of members of the smallest coalition, while the size and color of the dot indicates the size and mean ideology of this coalition. Background shading indicates whether Democrats (blue) or Republicans (red) held a majority in the chamber during the respective session.

ness = 4.49), Rep. Barney Frank (D-MA4, 4.02), and Rep. Daniel Glickman (D-KS4, 3.68). Similarly, the conservative-leaning third coalition during the Republican-controlled 106th–108th sessions (1999–2004) was anchored by Rep. Christopher Smith (R-NJ4, 8.44), Rep. Bill Young (R-FL10, 4.41), and Rep. Nancy Johnson (R-CT6, 2.98). Most recently, the conservative-leaning third coalition during the Republican-controlled 114th–115th sessions (2015–2018) was anchored by Rep. Edward Royce (R-CA39, 5.46), Rep. John Katko (R-NY24, 5.36), and Rep. Dave Reichert (R-WA8, 2.30).

Not only are members of the third coalition more effective than their traditional liberal and conservative coalition counterparts, but they also maintain distinctive political relations. Members of the traditional coalitions have 2.68 negative edges for every positive edge, but members of the third coalition have 21.18 negative edges for every positive edge (See *SI* Figure 7). Moreover, although 8.44% of traditional coalition members' negative edges are with co-partisans, over one-quarter (25.6%) of third coalition members' negative edges are with co-partisans.

Discussion

Optimally partitioning signed networks according to generalized balance theory is computationally challenging, but often essential to understanding their structure. In this paper, we have developed a solution to this challenge, both demonstrating its computational feasibility and highlighting the novel structural insights that the resulting optimal partitions can reveal. Specifically, we have developed a pair of optimization models that make it practical to partition a signed network into exactly k clusters that minimize the number of frustrated edges across all possible k-partitions (taking 3.3 hours on average for networks with up to $\sim 30,000$ edges using (1)), and to identify the smallest number of clusters that minimizes the number of frustrated edges across all possible partitions (taking 14 hours on average for networks with up to $\sim 30,000$ edges using (2)). Applying these models to signed networks of collaboration and opposition among legislators in the US House allowed us to determine that these relationships are not structured by legislators' political party affiliations, but instead by a three coalition system composed of a dominant liberal coalition, a dominant conservative coalition, and a previously obscured 'third coalition.' This hidden third coalition is noteworthy because its median ideology is unstable, however its members are consistently more effective at passing legislation than their colleagues in either of the dominant coalitions.

Just as community detection algorithms advanced the ability to uncover patterns in unsigned networks a decade ago [20], these models can advance the ability to uncover patterns in signed networks. However, unlike most community detection algorithms for which global optimization is not possible [40], our models guarantee an optimal signed network partition. These innovations are important because signed networks are already studied in a wide range of contexts including biology [1, 2, 3], finance [2, 4], politics [5, 21, 7], and psychology [41]. Moreover, statistical models now exist that enable signed networks to be constructed from virtually any empirical bipartite network data [42, 43], making signed networks available for analysis in a still broader range of contexts. The models we propose are perfectly general, but currently are practical for globally optimal partitioning of signed networks with up to $30,000$ edges. However, in practice this is only a minor limitation because most empirical signed networks contain fewer edges, and models for constructing signed networks include methods for sparsifying otherwise dense signed networks [43].

In addition to the methodological advances that our optimization models offer in the study of signed networks, our illustrative application of these models has also revealed a new way of thinking about how the US House of Representatives is organized. We observe that partitioning legislators into three coalitions according to generalized balance offers a better fit to their observed pattern of collaborations and oppositions than simply clustering them by political party. This suggests that the forces guiding coalition formation in the US House are more subtle and go beyond partisanship alone, even during periods of extreme polarization.

The previously obscured 'third coalition' we identified is unique in two important respects. First, members of the third coalition are highly effective at passing legislation, which has implications for how a party's majority status is interpreted. Although members of the majority

political party always appear to be more effective than members of the minority party, a substantial portion of this apparent majority advantage is conferred by the highly effective members of the third coalition, who tend to be ideologically aligned with the majority. Second, members of the third coalition have a much higher ratio of oppositions (negative edges) to collaborations (positive edges), and maintain more oppositions with members of their own party, which has implications for how membership in the third coalition is interpreted. These patterns suggest that although members of the third coalition may be ideologically aligned with the dominant coalition and majority party, they nonetheless represent a breakaway faction that are highly effective despite their rejection of partisanship. Our ability to identify such a cluster is noteworthy because it provides empirical support for earlier simulation studies suggesting that the introduction of independent legislators to an existing two-party legislature can increase the body's overall legislative effectiveness [44]. Although these simulation studies might have been viewed as hinting at a strategy for reinvigorating democratic systems plagued by partisanship, our findings suggest it may already be in place in the US House of Representatives.

Materials and Methods

We infer the collaboration and opposition patterns of legislators from their bill co-sponsorships [45, 46, 5]. These data begin as a bipartite network $\mathbf{B}$ in which legislators are connected to the bills they sponsor in a given session. From this, we construct the bipartite projection $\mathbf{P}$, which captures the number of bills each pair of legislators has co-sponsored together. Finally, we use the Stochastic Degree Sequence Model (SDSM) [46], implemented in the `backbone` package in R [43], to statistically infer a signed network of political collaboration and opposition. The SDSM applies a statistical test to the bipartite projection to yield a signed backbone $\mathbf{P}'$ in which there exists a positive (negative) edge between each pair of legislators who have co-sponsored statistically significantly more (fewer) bills than expected by chance. The random expectation is obtained from a canonical null model in which bill sponsorship is random, but expected values of both degree sequences of $\mathbf{B}$ are preserved. Because the SDSM involves performing a statistical test for each pair of legislators, we ensure a family-wise error rate of $\alpha = 0.01$ by applying a Holm-Bonferroni correction [47].

We measure legislators' ideology using 1$^{\text{st}}$ dimension Nokken-Poole ideology scores obtained from the Voteview database [48]. These scores are similar to the widely used DW-Nominate ideological scores [49, 50, 51], ranging from -1 (liberal) to 1 (conservative), except that they can vary across sessions. We measure legislators' effectiveness using legislative effectiveness scores provided by the Center for Effective Lawmaking at `https://thelawmakers.org/data-download`. These scores were computed from fifteen indicators constructed from the intersection of three types of bills (commemorative, substantive, or substantive and significant) and five stages of a bill's progression through the legislative life cycle (sponsored, committee action, post-committee action, chamber passage, and becoming law). These fifteen

indicators capture the effectiveness of a legislator to advance their agenda items using methods described by [37], and are normalized so that the mean effectiveness in each session is 1.

Acknowledgements: The authors are thankful to Aliakbar Akbaritabar, Sarah C. Johnson, Oul Han, and David Schoch for comments and discussions, which helped to improve this article.
Funding: There is no funding to be reported for this study.
Author Contributions: S.A. formulated mathematical models, used new methods to run experiments and solve models, combined and reconfigured data, obtained the results, and assisted in plotting and analyzing them; Z.P.N. developed new methods to infer network data, prepared plots, visualized the networks, and analyzed the results; both authors contributed to reviewing the literature, designing and conducting the research, and writing the paper.
Competing Interests: Authors declare that they have no competing interests.
Data availability: All the data and codes used in this study are publicly available with links and descriptions provided in the supplementary information.

References

[1] G. Iacono, F. Ramezani, N. Soranzo, C. Altafini, Determining the distance to monotonicity of a biological network: a graph-theoretical approach. *IET Systems Biology* **4**, 223–235 (2010).

[2] S. Aref, M. C. Wilson, Balance and frustration in signed networks. *Journal of Complex Networks* **7**, 163-189 (2019).

[3] A. Tahmassebi, B. Mohebali, L. Meyer-Baese, P. Solimine, K. Pinker, A. Meyer-Baese, *Smart Biomedical and Physiological Sensor Technology XVI*, B. M. Cullum, D. Kiehl, E. S. McLamore, eds., International Society for Optics and Photonics (SPIE, 2019), vol. 11020, pp. 53 – 60.

[4] P. C. Souto, A. S. Teixeira, A. P. Francisco, F. C. Santos, *International Conference on Complex Networks and their Applications* (Springer, Cham, Switzerland, 2018), pp. 534–546.

[5] Z. P. Neal, A sign of the times? Weak and strong polarization in the U.S. Congress, 1973–2016. *Social Networks* **60**, 103 - 112 (2020).

[6] S. Aref, L. Dinh, R. Rezapour, J. Diesner, Multilevel structural evaluation of signed directed social networks based on balance theory. *Scientific Reports* **10**, 1–12 (2020).

[7] D. Schoch, U. Brandes, Legislators' roll-call voting behavior increasingly corresponds to intervals in the political spectrum. *Scientific Reports* **10**, 1–9 (2020).

[8] J. A. Davis, Clustering and structural balance in graphs. *Human Relations* **20**, 181–187 (1967).

[9] D. Cartwright, F. Harary, *Social networks: Surveys, advances, and commentaries*, P. W. Holland, S. Leinhardt, eds. (Academic Press, 1976), pp. 25–50.

[10] V. Batagelj, Semirings for social networks analysis. *Journal of Mathematical Sociology* **19**, 53–68 (1994).

[11] P. Doreian, A. Mrvar, A partitioning approach to structural balance. *Social networks* **18**, 149–168 (1996).

[12] N. Bansal, A. Blum, S. Chawla, Correlation clustering. *Machine learning* **56**, 89–113 (2004).

[13] E. D. Demaine, D. Emanuel, A. Fiat, N. Immorlica, Correlation clustering in general weighted graphs. *Theoretical Computer Science* **361**, 172–187 (2006).

[14] S. Aref, A. J. Mason, M. C. Wilson, A modeling and computational study of the frustration index in signed networks. *Networks* **75**, 95-110 (2020).

[15] V. A. Traag, J. Bruggeman, Community detection in networks with positive and negative links. *Physical Review E* **80**, 036115 (2009).

[16] S. Gómez, P. Jensen, A. Arenas, Analysis of community structure in networks of correlated data. *Physical Review E* **80**, 016114 (2009).

[17] T. Zaslavsky, Balanced decompositions of a signed graph. *Journal of Combinatorial Theory, Series B* **43**, 1–13 (1987).

[18] S. Aref, A. J. Mason, M. C. Wilson, *Optimization Problems in Graph Theory*, B. Goldengorin, ed. (Springer, 2018), pp. 65–84.

[19] D. Sherrington, S. Kirkpatrick, Solvable model of a spin-glass. *Physical Review Letters* **35**, 1792–1796 (1975).

[20] S. Fortunato, Community detection in graphs. *Physics Reports* **486**, 75–174 (2010). ArXiv: 0906.0612.

[21] S. Aref, Z. P. Neal, Detecting coalitions by optimally partitioning signed networks of political collaboration. *Scientific Reports* **10**, 1–10 (2020).

[22] F. Heider, Social perception and phenomenal causality. *Psychological Review* **51**, 358-378 (1944).

[23] D. Cartwright, F. Harary, Structural balance: A generalization of Heider's theory. *Psychological Review* **63**, 277-293 (1956).

[24] G. C. Layman, T. M. Carsey, J. M. Horowitz, Party polarization in American politics: Characteristics, causes, and consequences. *Annual Review of Political Science* **9**, 83-110 (2006).

[25] Y. Zhang, A. J. Friend, A. L. Traud, M. A. Porter, J. H. Fowler, P. J. Mucha, Community structure in Congressional cosponsorship networks. *Physica A* **387**, 1705–1712 (2008).

[26] J. Moody, P. J. Mucha, Portrait of political party polarization. *Network Science* **1**, 119–121 (2013).

[27] F. Harary, J. A. Kabell, A simple algorithm to detect balance in signed graphs. *Mathematical Social Sciences* **1**, 131–136 (1980).

[28] M. Brusco, D. Steinley, K-balance partitioning: An exact method with applications to generalized structural balance and other psychological contexts. *Psychological Methods* **15**, 145–157 (2010).

[29] R. Figueiredo, G. Moura, Mixed integer programming formulations for clustering problems related to structural balance. *Social Networks* **35**, 639–651 (2013).

[30] L. Drummond, R. Figueiredo, Y. Frota, M. Levorato, *On the Move to Meaningful Internet Systems: OTM 2013 Workshops*, Y. T. Demey, H. Panetto, eds. (Springer, Berlin, Heidelberg, 2013), pp. 674–683.

[31] M. Levorato, L. Drummond, Y. Frota, R. Figueiredo, *Proceedings of the 30th Annual ACM Symposium on Applied Computing*, A. Bechini, J. Hing, eds., SAC '15 (ACM, NY, USA, 2015), pp. 1117–1122.

[32] M. Levorato, R. Figueiredo, Y. Frota, L. Drummond, Evaluating balancing on social networks through the efficient solution of correlation clustering problems. *EURO Journal on Computational Optimization* **5**, 467–498 (2017).

[33] Gurobi Optimization Inc., Gurobi optimizer reference manual (2020). Url: `http://gurobi.com/documentation/9.1/refman/index.html` date accessed 1 December 2020.

[34] C. Andris, D. Lee, M. J. Hamilton, M. Martino, C. E. Gunning, J. A. Selden, The rise of partisanship and super-cooperators in the U.S. House of Representatives. *PLOS One* **10**, 1–14 (2015).

[35] D. M. Olson, C. T. Nonidez, Measures of legislative performance in the U.S. House of Representatives. *Midwest Journal of Political Science* **16**, 269–277 (1972).

[36] S. Frantzich, Who makes our laws? The legislative effectiveness of members of the U.S. Congress. *Legislative Studies Quarterly* **4**, 409–428 (1979).

[37] C. Volden, A. E. Wiseman, *Legislative effectiveness in the United States Congress: The lawmakers* (Cambridge University Press, 2014).

[38] D. W. Moore, Legislative effectiveness and majority party size: A test in the Indiana House. *The Journal of Politics* **31**, 1063–1079 (1969).

[39] D. R. Mayhew, *Divided we govern: Party control, lawmaking, and investigations, 1946-2002* (Yale University Press, 2005).

[40] A. Lancichinetti, S. Fortunato, Limits of modularity maximization in community detection. *Physical review E* **84**, 066122 (2011).

[41] L. F. Bringmann, T. Elmer, S. Epskamp, R. W. Krause, D. Schoch, M. Wichers, J. T. Wigman, E. Snippe, What do centrality measures measure in psychological networks? *Journal of Abnormal Psychology* **128**, 892 (2019).

[42] S. Epskamp, E. I. Fried, A tutorial on regularized partial correlation networks. *Psychological methods* **23**, 617 (2018).

[43] R. Domagalski, Z. P. Neal, B. Sagan, Backbone: An R package for extracting the backbone of bipartite projections. *PLOS One* **16**, 1-20 (2021).

[44] A. Pluchino, C. Garofalo, A. Rapisarda, S. Spagano, M. Caserta, Accidental politicians: How randomly selected legislators can improve parliament efficiency. *Physica A: Statistical Mechanics and its Applications* **390**, 3944-3954 (2011).

[45] J. H. Fowler, Legislative cosponsorship networks in the US House and Senate. *Social Networks* **28**, 454–465 (2006).

[46] Z. P. Neal, The backbone of bipartite projections: Inferring relationships from co-authorship, co-sponsorship, co-attendance and other co-behaviors. *Social Networks* **39**, 84–97 (2014).

[47] S. Holm, A simple sequentially rejective multiple test procedure. *Scandinavian Journal of Statistics* **9**, 65–70 (1979).

[48] J. B. Lewis, K. T. Poole, H. Rosenthal, A. Boche, A. Rudkin, L. Sonnet, Voteview: Congressional roll-call votes database (2020). Accessed 9 October 2020.

[49] K. T. Poole, H. Rosenthal, The polarization of American politics. *The Journal of Politics* **46**, 1061–1079 (1984).

[50] K. T. Poole, H. Rosenthal, *Congress: A political-economic history of roll call voting* (Oxford University Press, 2000).

[51] G. W. Cox, K. T. Poole, On measuring partisanship in roll-call voting: The US House of Representatives, 1877-1999. *American Journal of Political Science* **46**, 477–489 (2002).

[52] F. Hüffner, N. Betzler, R. Niedermeier, Separator-based data reduction for signed graph balancing. *Journal of Combinatorial Optimization* **20**, 335–360 (2010).

[53] G. Facchetti, G. Iacono, C. Altafini, Computing global structural balance in large-scale signed social networks. *Proceedings of the National Academy of Sciences* **108**, 20953–20958 (2011).

[54] G. Facchetti, G. Iacono, C. Altafini, Exploring the low-energy landscape of large-scale signed social networks. *Physical Review E* **86**, 036116 (2012).

[55] L. Li, Y. Fan, A. Zeng, Z. Di, Binary opinion dynamics on signed networks based on Ising model. *Physica A: Statistical Mechanics and its Applications* **525**, 433-442 (2019).

[56] F. Harary, M.-H. Lim, D. C. Wunsch, Signed graphs for portfolio analysis in risk management. *IMA Journal of Management Mathematics* **13**, 201–210 (2002).

[57] P. Doreian, A. Mrvar, Structural Balance and Signed International Relations. *Journal of Social Structure* **16**, 1-49 (2015).

[58] T. Derr, J. Tang, *2018 IEEE International Conference on Data Mining Workshops (ICDMW)* (IEEE, 2018), pp. 1501–1502.

[59] N. Arınık, R. Figueiredo, V. Labatut, Multiple partitioning of multiplex signed networks: Application to European parliament votes. *Social Networks* **60**, 83–102 (2020).

[60] N. Arınık, R. Figueiredo, V. Labatut, Multiplicity and diversity: analysing the optimal solution space of the correlation clustering problem on complete signed graphs. *Journal of Complex Networks* **8** (2021).

Supplementary information

Supplementary Text
Figs. 5 to 7
Tables 1 to 2
Movie S1
Databases S1 to S2
References (52–60)

Supplementary information for **optimally partitioning signed networks based on generalized balance**

Supplementary Text

Data and code availability

All network data, numerical results, and replication code related to this study are publicly available with links provided in this document. The R code and the processed data for analyzing and visualizing the results are publicly available on an OSF repository at `https://doi.org/10.17605/OSF.IO/3QTFB`.

Solving the graph optimization models

The proposed optimization models can be solved by mathematical programming solvers which supports 0/1 linear programming (binary linear) models. The code for both optimization models will be made available on a GitHub repository at `https://github.com/saref/clusterability-index` once this paper is published. In the GitHub repository, we provide Python code for using Gurobi solver (version 9.1) to solve the proposed binary linear models and obtain optimal partitions of signed networks into internally cohesive and mutually divisive clusters based on generalized balance theory.

Using Gurobi for solving the proposed optimization models

Our proposed algorithms are developed in Python 3.8 based on the mathematical programming models discussed in the paper which partition signed networks based on generalized balance into an optimal k-partition or an optimal partition without specifying k.

These optimization algorithms are distributed under an Attribution-NonCommercial-ShareAlike 4.0 International (CC BY-NC-SA 4.0) license. This means that one can use these algorithms for non-commercial purposes provided that they provide proper attribution for them by citing the current article. Copies or adaptations of the algorithms should be released under the similar license.

The following steps outline the process for academics to install the required software (*Gurobi* solver [33]) on your computer to be able to run the optimization algorithms:

1. Download and install Anaconda (Python 3.8 version) which allows you to run a Jupyter code. It can be downloaded from `https://anaconda.com/products/individual`. Note that you must select your operating system first and download the corresponding installer.

2. Register for an account on `https://pages.gurobi.com/registration` to get a free academic license for using Gurobi. Note that Gurobi is a commercial software, but it can be registered with a free academic license if the user is affiliated with a recognized degree-granting academic institution. This involves creating an account on Gurobi website to be able to request a free academic license in step 5.

3. Download and install Gurobi Optimizer (versions 9.1 and above are recommended) which can be downloaded from `gurobi.com/downloads/gurobi-optimizer-eula/` after reading and agreeing to Gurobi's End User License Agreement.

4. Install Gurobi into Anaconda. You do this by first adding the Gurobi channel to your Anaconda channels and then installing the Gurobi package from this channel.

   From a terminal window issue the following command to add the Gurobi channel to your default search list

   ```
   conda config --add channels

   http://conda.anaconda.org/gurobi
   ```

   Now issue the following command to install the Gurobi package

   ```
   conda install gurobi
   ```

5. Request an academic license from `https://pages.gurobi.com/registration` and install the license on your computer following the instructions given on Gurobi license page.

Completing these steps is explained in the following links (for version 9.1).
for Windows:
`https://www.gurobi.com/documentation/9.1/quickstart_windows/index.html`, for Linux:
`https://www.gurobi.com/documentation/9.1/quickstart_linux/index.html`, and for Mac:
`https://www.gurobi.com/documentation/9.1/quickstart_mac/index.html`.

After following the instructions above, open Jupyter Notebook which takes you to an environment (a new tab on your browser pops up on your screen) where you can open the main code (which is a file with .ipynb extension).

Visualization of 3-partition coalitions in selected House networks (Figures 5 and 6)

Fig. 5 shows the 3-partition coalitions in the 101^{st}, when the third coalition was dominated by highly effective ideologically liberal legislators. Fig. 6 shows the 3-partition coalitions in the 108^{th}, when the third coalition was dominated by highly effective ideologically conservative legislators. In both cases, green (positive) and red (negative) edges represent significantly many and significantly few co-sponsorships respectively. Node color indicates the legislator's ideology on a blue (liberal, Nokken-Poole = -1), purple (moderate, 0), red (conservative, +1) spectrum. Node size indicates the legislator's effectiveness. All nodes are labeled with legislators' names, which are visible when the figure is viewed at $400^{+}\%$ magnification.

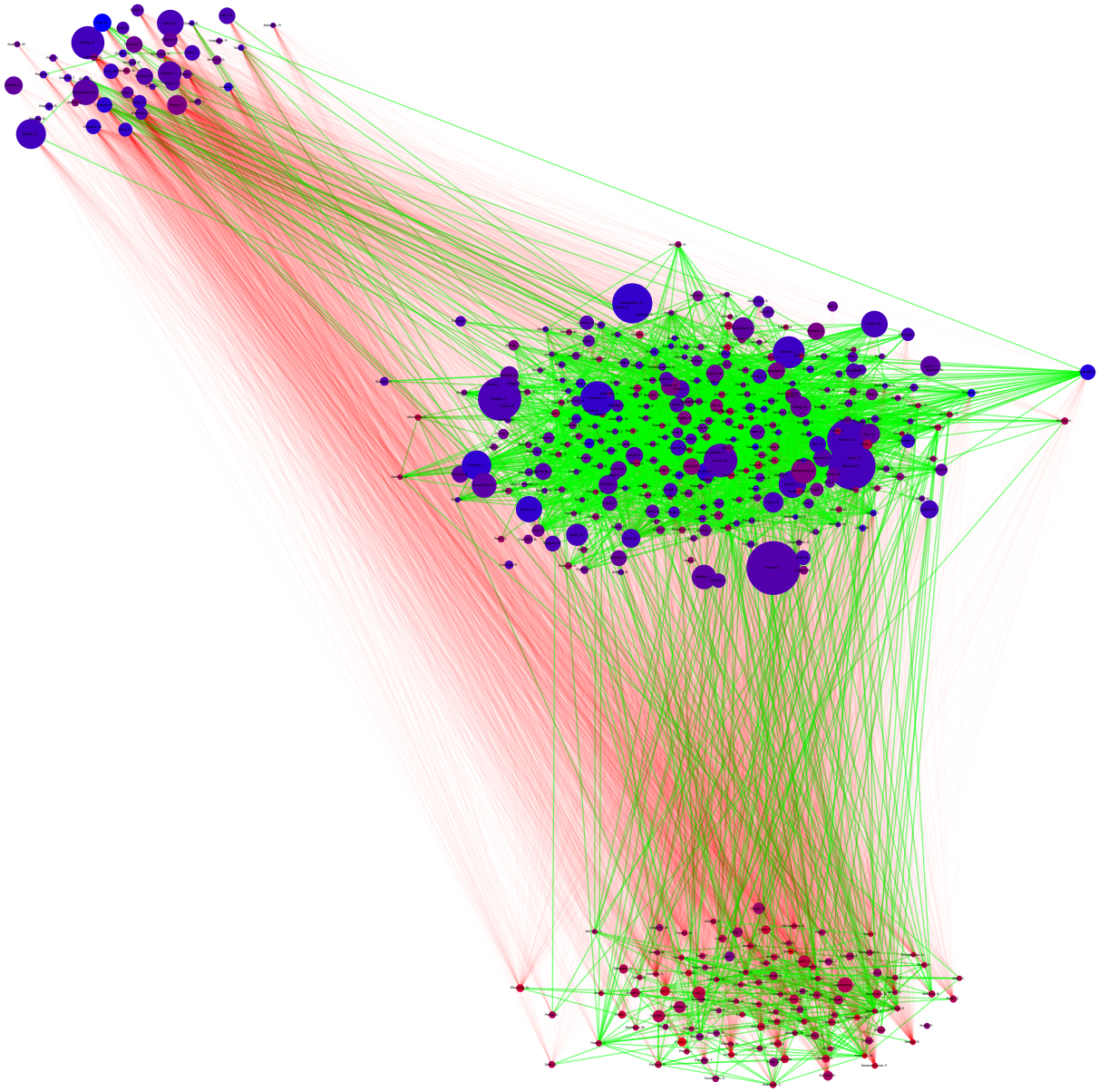


Figure 5: The 3-partition coalitions in the 101st session of the House of Representatives

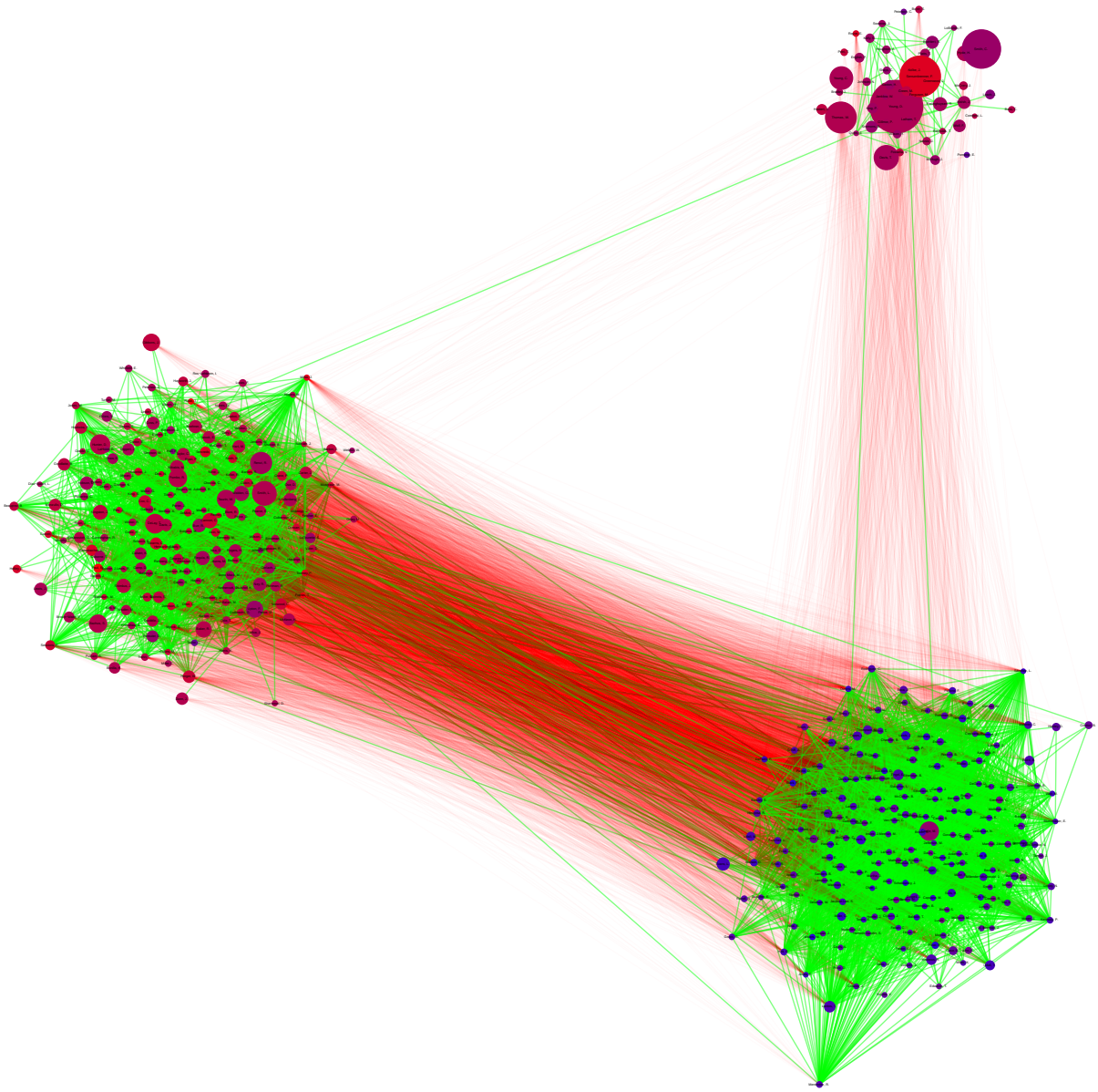


Figure 6: The 3-partition coalitions in the 108th session of the House of Representatives

Significance, generalizability, and limitations of our methods

The computational results we provided have broad relevance because they demonstrate the practical feasibility of solving fundamental NP-hard signed graph partitioning problems. Solving these partitioning problems are essential for exact evaluations of the structure of signed networks which go beyond the political science application we have demonstrated and have use cases in other fields from biology and physics [1, 52, 53, 54, 3, 55] to social sciences [56, 57, 4, 58, 5, 21, 59, 6, 7]. Specifically, our methods for partitioning a signed graph according to generalized balance improve upon heuristic methods that are fast but do not generally yield optimal partitions [30, 31, 32]. Additionally, our methods also improve upon existing methods for obtaining optimal partitions, but that are feasible only for small graphs where $n \leq 40$ [28, 29]. The correctness of our methods for partitioning signed networks is guaranteed by the branch and bound algorithm of Gurobi [33] which is an exact method for solving binary linear programming models to global optimality.

The instances we have solved to global optimality are considerably large and therefore generalize to a wide variety of other use cases with networks of up to $\sim 30,000$ edges. For example, the network of the 115^{th} session has $n = 448$ nodes, $m = 31,936$ edges and $|T| = 14,885,696$ connected triads. Obtaining an optimal 7-partition using Eq. 1 leads to an optimization model with $nk + m = 35,072$ binary variables and $mk + n = 224,000$ constraints, which takes Gurobi [33], 1.66 hours to solve. Moreover, obtaining an optimal partition (without specifying k) using Eq. 2 leads to an optimization model with $n(n-1)/2 = 100,128$ binary variables and $3|T| = 44,657,088$ constraints, which takes Gurobi [33] only 5.28 hours to solve. While obtaining these partitions requires a few hours, the resulting partition is guaranteed to be globally optimal, which is essential for an exact evaluation of the structure of signed graphs.

The main limitation of the models in Eqs. 1–2 (in the manuscript) is the size of the network they can handle in a reasonable time. We have demonstrated the practicability of these models for networks with up to $\sim 30,000$ edges considering that a few hours is worth finding a globally optimal solution for the exact evaluation of the structure of the network. From a practical standpoint, two factors are relevant for determining whether these computationally intensive models are suitable for a different use case: network properties and processing capabilities. Previous studies suggest that some properties of the input graph like degree heterogeneity could be determinant factors of solve time in similar problems [14]. Also, structural regularities in networks constructed from empirical data make them easier to solve compared to synthetic networks (like random graphs) [14]. As Gurobi solver makes use of multiple processing threads to explore the feasible space in parallel, the processing capabilities of the computer that runs the optimization solver could also make an impact.

The computing processor configuration we have used (32 Intel Xeon CPU E7-8890 v3 @ 2.50 GHz processors) and the size of the real networks we have analyzed ($m \sim 30,000$) have led to solve times of roughly a few hours per instance. One could speculate that larger networks on the same hardware or the same networks on less powerful hardware is expected to take longer. In such cases, one may consider using a non-zero optimality gap tolerance (*MIPGap* as

a Gurobi parameter [33]) to find solutions within a guaranteed proximity of optimality to reduce the solve time.

Multiplicity of optimal solutions

There are symmetries in the mathematical formulations for the two models in Eqs. 1–2 (in the manuscript). For example, in Eq. 1, a given 2-partition can be expressed by different feasible solutions (sets of values for decision variables). This is because the clusters are treated indifferently and could be swapped while the partition remains virtually unchanged. As another example, in Eq. 2, a feasible solution does not necessarily represent a unique partition. This is due to the original formulation [13] in which a pair of non-adjacent nodes a and i may have no decision variables indicating they belong to the same cluster with any of their neighbours (denoted by b and j respectively $\forall b, j : a_{ab} \neq 0, a_{ij} \neq 0$) i.e. all the decision variables associated with a and i take the value zero. In that case, the same feasible solution could lead to two partitions (with identical fitness) depending on whether nodes a and i are placed in the same or different clusters. Another source of symmetry is the existence of isolate nodes whose optimal cluster membership is random and therefore not meaningful. When characterizing the composition of clusters in our analyses, we have ignored isolates.

Due to the symmetries outlined above, both optimization models in Eqs. 1–2 generally have multiplicity in their optimal solutions. Finding all optimal solutions to such computationally intensive problems are not practically feasible for large instances. For small instances, however, previous studies have looked at multiplicity of optimal solutions in similar partitioning problems [6, 60]. Although optimal 2-partitions can be unique in some small real-world signed networks [6], more often multiple optimal solutions exist [6, Fig. S1 in]. Also, in the case of small complete random signed graphs, multiple optimal solutions may exist [60]. Due to the practical complexity of these problems and the size of empirical networks we consider, although we cannot find and analyze all optimal partitions, it is certain that the optimal partitions are not unique. Future work is needed to find practical methods for finding and analyzing all optimal partitions of such large networks.

Oppositional ties of the splinter coalition

Members of the third coalition have 21.18 negative ties for every positive tie which is substantially different from the members of traditional coalitions who have on average 2.68 negative ties for every positive tie. This distinction in oppositional ties deserves more attention and we look at the fraction of each type of edge by coalition, taking into account the party of legislator at the other endpoint of the edge.

Figure 7 illustrates the fractions of positive and negative edges with co-partisans (members of the same party) for each of the coalitions based on the optimal 3-partitions. Fractions of positive (negative) edges are shown by solid (dashed) lines. The red, blue, and green lines represent the conservative coalition, the liberal coalition, and the splinter coalition respectively.

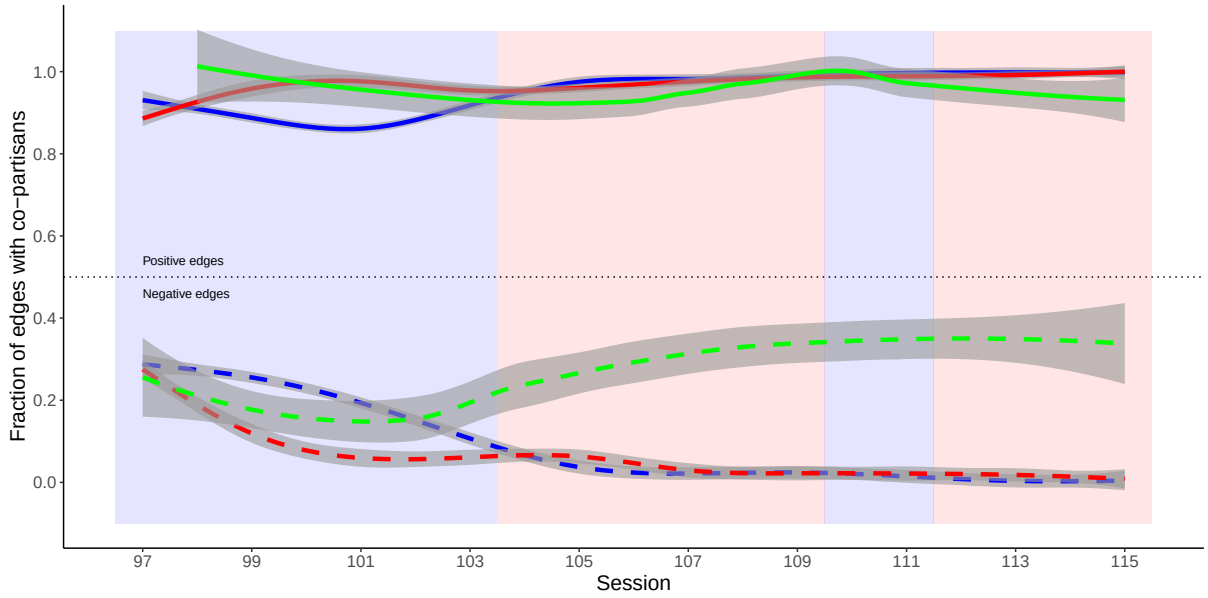


Figure 7: Fractions of positive and negative edges to members of the same party aggregated for each of the three coalitions

It can be seen in Figure 7 that the three coalitions are similar based on the fraction of positive edges with co-partisans: members of all coalitions mainly collaborate (i.e. have a positive edge with) members of their own party. For the fraction of negative edges with co-partisans, however, the splinter coalition shifts away from the main liberal and conservative coalition. From the 104^{th} session, this quantity has generally increased for the splinter coalition reaching values close to 0.4. This means that legislators in the splinter coalitions have a considerable proportion (nearly 40%) of their negative edges with members of the own party. Given this distinctive feature in oppositional ties, one may conclude that the members of the third coalition are distinctively more willing to push back against their own party.

Additional numerical results (Tables 1 to 2)

Table 1: Detailed properties and clusterability indices for networks

Session	Start year	n	m	density	m^-	m^+	m^-/m	$C_2(G)$	$C_3(G)$	$C_4(G)$	$C_5(G)$	$C_6(G)$	$C_7(G)$	$C(G)$
97	1981	447	4954	0.05	4494	460	0.91	280	36	14	6	**4**	**4**	**4**
98	1983	444	6744	0.07	5460	1284	0.81	435	102	60	49	45	**44**	**44**
99	1985	443	8714	0.07	6759	1955	0.78	962	79	48	40	**38**	**38**	**38**
100	1987	446	8520	0.08	6888	1632	0.81	560	118	89	**84**	**84**	**84**	**84**
101	1989	449	10180	0.10	7970	2210	0.78	896	263	207	188	**183**	**183**	**183**
102	1991	447	13692	0.11	10152	3540	0.74	748	169	119	112	**111**	**111**	**111**
103	1993	446	13281	0.10	10530	2751	0.79	301	245	**241**	**241**	**241**	**241**	**241**
104	1995	445	13019	0.13	10301	2718	0.79	17	**7**	**7**	**7**	**7**	**7**	**7**
105	1997	449	16709	0.13	13125	3584	0.79	50	22	**16**	**16**	**16**	**16**	**16**
106	1999	442	17746	0.14	13390	4356	0.75	91	48	40	**39**	**39**	**39**	**39**
107	2001	447	17908	0.14	14062	3846	0.79	59	34	**31**	**31**	**31**	**31**	**31**
108	2003	444	19384	0.16	14211	5173	0.73	63	33	**29**	**29**	**29**	**29**	**29**
109	2005	445	21601	0.17	15684	5917	0.73	69	44	35	**34**	**34**	**34**	**34**
110	2007	452	23719	0.15	17094	6625	0.72	44	31	**30**	**30**	**30**	**30**	**30**
111	2009	451	21564	0.21	15342	6222	0.71	153	87	82	**78**	**78**	**78**	**78**
112	2011	450	29904	0.19	21118	8786	0.71	39	30	**28**	**28**	**28**	**28**	**28**
113	2013	447	25992	0.21	19026	6966	0.73	24	20	**18**	**18**	**18**	**18**	**18**
114	2015	446	30149	0.22	21299	8850	0.71	57	38	**37**	**37**	**37**	**37**	**37**
115	2017	448	31936	0.32	21883	10053	0.69	221	38	**35**	**35**	**35**	**35**	**35**

Cases indicating the stagnation of frustrated edges are shown in bold-face font.

Table 2: The size and effectiveness of the two parties and optimal 3-partition coalitions

	Partition based on political party						**Generalized Balance Partition** ($k = 3$)								
	Size		Median Ideology		Mean Effectiveness		Size			Median Ideology			Mean Effectiveness		
session	D	R	D	R	D	R	L	C	S	L	C	S	L	C	S
97	245	194	-0.33	0.28	1.45	0.44	153	255	18	-0.40	0.20	0.29	1.29	0.83	1.59
98	272	167	-0.32	0.32	1.37	0.39	288	99	51	-0.22	0.32	-0.37	1.05	0.55	1.55
99	256	182	-0.32	0.34	1.45	0.37	304	85	47	-0.19	0.41	-0.41	1.07	0.40	1.70
100	261	179	-0.33	0.35	1.40	0.43	282	125	29	-0.28	0.39	-0.34	1.09	0.54	2.31
101	264	179	-0.33	0.35	1.41	0.40	290	105	45	-0.22	0.42	-0.37	1.10	0.40	1.70
102	270	170	-0.33	0.34	1.40	0.39	299	100	37	-0.24	0.41	-0.36	1.11	0.42	1.94
103	259	180	-0.34	0.38	1.45	0.32	224	176	32	-0.36	0.38	-0.21	1.53	0.35	0.89
104	207	231	-0.38	0.38	0.33	1.60	140	258	22	-0.44	0.36	-0.31	0.31	1.39	0.49
105	211	231	-0.39	0.39	0.33	1.62	194	208	32	-0.40	0.41	0.15	0.40	1.50	1.23
106	212	224	-0.39	0.39	0.39	1.58	210	182	42	-0.39	0.43	0.23	0.41	1.41	2.21
107	213	228	-0.39	0.38	0.41	1.54	204	202	30	-0.39	0.40	0.24	0.44	1.42	1.96
108	208	230	-0.39	0.41	0.40	1.53	205	186	46	-0.39	0.43	0.29	0.43	1.27	2.38
109	203	236	-0.38	0.41	0.48	1.51	210	210	15	-0.38	0.42	0.25	0.48	1.46	1.63
110	241	206	-0.38	0.43	1.45	0.45	242	195	8	-0.38	0.44	0.12	1.43	0.44	0.69
111	263	182	-0.37	0.47	1.36	0.44	195	176	69	-0.42	0.47	-0.18	1.34	0.44	1.42
112	198	245	-0.40	0.47	0.47	1.42	178	250	9	-0.41	0.46	0.29	0.47	1.33	1.75
113	203	238	-0.40	0.48	0.51	1.42	197	236	4	-0.41	0.48	0.06	0.52	1.43	0.34
114	188	249	-0.40	0.49	0.58	1.32	186	242	8	-0.40	0.50	0.21	0.58	1.28	2.20
115	195	243	-0.39	0.49	0.59	1.35	192	211	33	-0.39	0.52	0.24	0.59	1.27	1.80

In party-partition: D = Democratic coalition, R = Republican coalition

In 3-partition: L = Liberal coalition, C = Conservative coalition, S = Splinter coalition

Movie S1: Slideshow of the 3-partition coalitions of the signed US House networks

A slideshow of optimal 3-partition coalitions is available online at `https://saref.github.io/SI/AN2021/House_coalitions.mp4` which includes all 19 House networks. As in Figures 5 and 6, green and red edges represent significantly many and significantly few cosponsorships respectively. Node color indicates the legislator's ideology on a blue (liberal, Nokken-Poole = -1), purple (moderate, 0), red (conservative, +1) spectrum. Node size indicates the legislator's effectiveness. Looking at the colors and positions of edges we can see that the large majority of edges are intra-cluster positive or inter-cluster negative. In these networks, only 0.05%–2.5% of the edges are frustrated under the optimal 3-partitions which indicate the closeness of the networks to the assertions of the generalized balance theory [8]. If we look at the colors of the nodes, we see the ideological divide between the members of different coalitions. The splinter coalition is the smallest cluster of the nodes which usually has several large nodes (highly effective legislators).

Dataset S1: frustrated_legislators.RData and frustrated_legislators.R on OSF

The file 'frustrated_legislators.RData' is an R workspace which includes a dataframe object 'data' that contains details about each legislator in each session (e.g. ideology, effectiveness, cluster membership in optimal k-partitions), and 19 igraph objects 'H###' that contain signed networks for each session. The file 'frustrated_legislators.R' in the same repository contains the R code to replicate all substantive analyses reported in the manuscript using these data. Both files are publicly available at `https://doi.org/10.17605/OSF.IO/3QTFB`. The data are distributed under a CC-BY 4.0 license, which means that they can be used provided they are properly attributed by citing [5, 43] and the current article.

Dataset S2: clusters-house.csv

The results on globally optimal solutions to the optimization model for k-partitioning House networks are available in comma-separated values format at `https://saref.github.io/SI/AN2021/clusters-house.csv`. The first and second columns contain session numbers and legislator name as indicated by the headers. Each row is a legislator-session combination. The other columns are the cluster assignments based on optimal k-partitions for $k \in \{2, 3, \ldots, 7\}$ as indicated by the column header. The entries represent the cluster assignment of the node associated to the row (the legislator-session combination) based on an optimal solution of the k-partition associated to the column.